THE HOMOLOGICAL ARROW POLYNOMIAL FOR VIRTUAL LINKS

KYLE A. MILLER

Abstract. The arrow polynomial is an invariant of framed oriented virtual links that generalizes the virtual Kauffman bracket. In this paper we define the *homological arrow polynomial*, which generalizes the arrow polyomial to framed oriented virtual links with labeled components. The key observation is that, given a link in a thickened surface, the homology class of the link defines a functional on the surface's skein module, and this gives an invariant of the link itself by applying it to the image of the link in the skein module — this is the arrow polynomial.

We give a graphical calculus for the homological arrow polynomial by introducing labeled "whiskers" to the usual diagrams for the Kauffman bracket, recording intersection numbers with each labeled component of the link.

We use the homological arrow polynomial to study $(\mathbb{Z}/n\mathbb{Z})$-nullhomologous virtual links and checkerboard colorability, completing Imabeppu's characterization of checkerboard colorability of virtual links with up to four crossings. We also prove a version of the Kauffman–Murasugi–Thistlethwaite theorem that the breadth of the homological arrow polynomial for an "h-reduced" diagram is four times the difference between the crossing number and the genus of the diagram.

Contents

1. Introduction

sec:introduction

A *surface link* is a link L in the interior of a thickened surface $\Sigma \times I$ up to isotopy, where Σ is a compact oriented surface, possibly with nonempty boundary. Given a compact subsurface $\Sigma' \subseteq \Sigma$, then the surface link $L \subset \Sigma' \times I$ is called a *destabilization* of $L \subset \Sigma \times I$. A *virtual link* is an equivalence class of surface links modulo destabilization [CKS02, Kup03]. Combinatorially, a virtual link can be given as a *virtual link diagram*, which is a ribbon graph where every vertex has degree

Date: —, 2020.

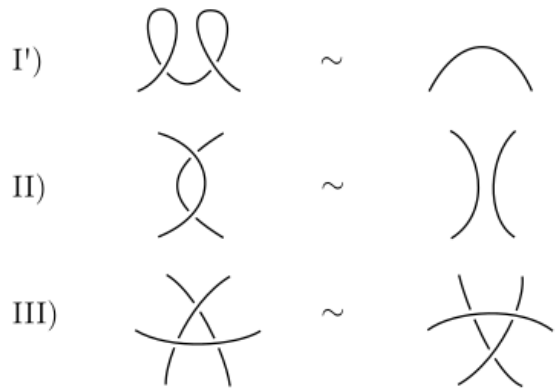

FIGURE 1. Reidemeister moves for framed surface links. fig:framed-reidemeister

2 or 4, where the degree-4 vertices have a marked pair of opposite half-edges corresponding to the overstrand of a crossing. Virtual link diagrams are usually immersed in the plane, and double points — artefacts of non-planarity — are called *virtual crossings*. Such diagrams up to the classical Reidemeister moves and *detour moves* (re-immersions of the ribbon graph) generate virtual equivalence [Kau99].

A *framed* surface link is a surface link $L \subset \Sigma \times I$ along with an extension to an embedding of $L \times I$ (not respecting the product structure of $\Sigma \times I$) up to isotopy. By extension, a *framed* (or *flat*) virtual link is an equivalence class of framed surface links modulo destabilization. Diagrammatically, the framing annuli are assumed to lie parallel to the plane, and the only change is that the Reidemeister I move is replaced by the Reidemeister I' move for regular isotopy (see Figure 1).

Discovered independently by Dye–Kauffman [DK09] and Miyazawa [Miy06, Miy08], the arrow polynomial is an invariant of oriented framed virtual links that takes values in $\mathbb{Z}[A^{\pm 1}, K_1, K_2, \dots]$. In the Dye–Kauffman formulation, the Kauffman bracket is modified to make use of the orientation of the virtual link by introducing cusps in the B-smoothing (see Figure 2). The evaluation of a fully resolved state as an element of the polynomial ring is from counting cusps after cusp cancelation rules. To explain this process we use the Miyazawa formulation. First, replace the cusps with *vertex orientations* according to Figure 3; these are local orientations at a degree-2 vertex labeled by an integer. Second, reduce the vertex orientations according to Figure 4, leaving a single vertex orientation along each component of the state. Third, evaluate the state as $(-A^2 - A^{-2})^{b_0(S)-1} \prod_{C \subseteq S} K_{|n(C)|/2}$, where $b_0(S)$ is the number of components in the state S, C ranges over components of the state, $n(C)$ is the label of the sole vertex orientation along that component (which is always even, as we will come to see), and $K_0 = 1$. Hence, the arrow polynomial is given by

$$\langle L \rangle_{\mathrm{A}} = \sum_S A^{a(S)-b(S)} (-A^2 - A^{-2})^{b_0(S)-1} \prod_{C \subseteq S} K_{|n(C)|/2}, \tag{1.1}$$

where $a(S)$ and $b(S)$ denote the number of A-smoothings and B-smoothings in state S.

For virtual links in general, Dye and Kauffman define the writhe-normalized arrow polynomial $\langle L \rangle_{NA} = (-A^3)^{-\mathrm{wr}(L)} \langle L \rangle_{\mathrm{A}}$, where the *writhe* is the sum of the signs of the crossings of the virtual link diagram. Said another way, the writhe-normalized arrow polynomial is the arrow polynomial of a writhe-0 representative in the equivalence class of framed virtual links modulo the usual Reidemeister I move. One might define the arrow version of the virtual Jones polynomial by substituting $t = A^{-4}$ in $\langle L \rangle_{NA}$. The usual virtual Jones polynomial, then, is from additionally setting $K_n = 1$ for all n.

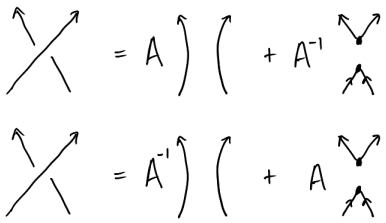

FIGURE 2. Crossing resolutions for the Dye–Kauffman arrow bracket, which introduce cusps. fig:arrow-bracket-1

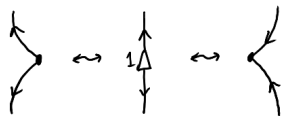

FIGURE 3. Graphical notation for cusps. fig:arrow-bracket-cusps

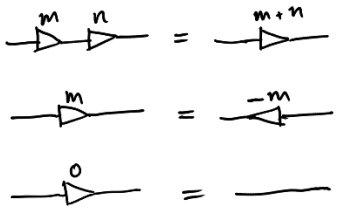

FIGURE 4. Cusp reduction rules using labeled vertex orientations. fig:arrow-bracket-cusp-reduction

In this paper, we give a formulation of the arrow polynomial from a homological point of view, similar in flavor to Turaev's two-variable extension of the Jones polynomial to knotoids [Tur]. This makes certain known observations about the arrow polynomial transparent while also giving a straightforward extension to virtual links in a way that distinguishes components.

While it is true a virtual link is represented as a surface link and so we may consider that link as an element in the Kauffman bracket skein module for the thickened surface, to get a polynomial invariant we need some linear functional on the skein module that is invariant under stabilization — this includes the action of the mapping class group. The basic idea is that the components of the surface link itself may be used as a marking to construct such a functional, and this leads to our virtual link invariant, where the one-component version of which is equivalent to the arrow polynomial.

When referring to virtual knots, we use Jeremy Green's census [Gre04]. For identification of virtual knots, we use the online software Virtual KnotFolio [Mil20].

2. The homological arrow polynomial

We will first consider framed oriented surface links in a fixed thickened surface $\Sigma \times I$, define a functional on the skein module of $\Sigma \times I$, and then show the result is an invariant under stabilization of the surface and hence of the corresponding virtual link.

The *Kauffman bracket skein module* $\mathrm{Sk}(M)$ for a 3-manifold M consists of $\mathbb{Z}[A^{\pm 1}]$-linear combinations of framed unoriented links in M, called *skeins*, modulo the relations for the Kauffman

bracket:

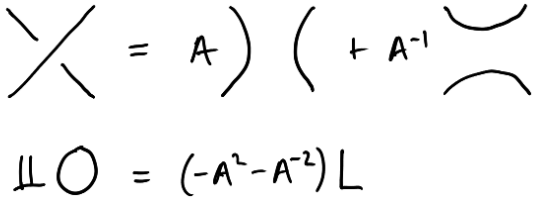

In the second relation, the unknot bounds a disk in M disjoint from L. The skein module $\mathrm{Sk}(\Sigma) := \mathrm{Sk}(\Sigma \times I)$ has a $\mathbb{Z}[A^{\pm 1}]$-algebra structure, where the multiplication operation is from including the first skein in $\Sigma \times [\frac{1}{2}, 1]$ and the second in $\Sigma \times [0, \frac{1}{2}]$. See [Prz].

Consider the ring $\mathcal{H}(\Sigma) = \mathbb{Z}[A^{\pm 1}][X_{\pm\gamma} : \gamma \in H_1(\Sigma)]/(X_0 = 1)$, where the $\pm\gamma$ indicates that the variables are associated to unoriented homology classes — note that we may restrict this to those γ that are represented by simple closed curves in what follows.

Lemma 2.1. *The ring $\mathcal{H}(\Sigma)$ has a well-defined structure of a $\mathrm{Sk}(\Sigma)$-module such that simple closed curves $C \subset \Sigma$ act by scaling by $(-A^2 - A^{-2})X_{\pm[C]}$, where $\pm[C]$ is the unoriented homology class of C.*

Proof. Given a framed link diagram L in Σ, then by applying the Kauffman bracket skein relation one can represent its value in $\mathrm{Sk}(\Sigma \times I)$ as a linear combination of *simple skeins*, which are disjoint unions of simple closed curves in $\Sigma \times \{1/2\}$, and as usual the decomposition into simple skeins is given by a state sum. The hypothesized module structure extends to L by the following state sum that gives the multiplicative factor for the action:

{eq:state-sum}
$$L \mapsto \sum_S A^{a(S)-b(S)}(-A^2 - A^{-2})^{b_0(S)} \prod_{C \in S} X_{\pm[C]}, \tag{2.1}$$

where the sum ranges over states for L. What remains is to show this multiplicative factor is invariant under the framed Reidemeister moves (Figure 1). Note that in the above state sum, nullhomologous $C \in S$ have $\pm[C] = 0$ and hence evaluate to $-A^2 - A^{-2}$. Thus, the usual check that the Kauffman bracket is invariant under framed Reidemeister moves carries over to this new state sum, and we are done. □

With this $\mathrm{Sk}(\Sigma)$-module in hand, we get a framed oriented surface link invariant, which is the amount by which it scales $\mathcal{H}(\Sigma)$. In particular, the invariant is given by Equation (2.1). This invariant is very similar to the surface bracket polynomial in [DK], however we expand homology classes multiplicatively in the additional variables.

Given homology classes $\lambda_1, \dots, \lambda_n \in H_1(\Sigma)$, there is a homomorphism $h : H_1(\Sigma) \to \mathbb{Z}^n$ defined by $\alpha \mapsto (\lambda_1 \cdot \alpha, \dots, \lambda_n \cdot \alpha)$ where $\lambda_i \cdot \alpha$ is the algebraic intersection number whose value lies in $H_0(\Sigma) \cong \mathbb{Z}$. The case we are interested in is from an oriented link L with components labeled by elements of $\{1, 2, \dots, n\}$, allowing different components to have the same label. We may regard a labeling as a disjoint union $L = L_1 \sqcup \cdots \sqcup L_n$ with L_i consisting of those components of L with label i, if any. Then, with $\lambda_i = [\pi(L_i)]$ for each i, we define $h_L : H_1(\Sigma) \to \mathbb{Z}^n$ as above, where $\pi : \Sigma \times I \to \Sigma$ is the canonical projection.

For an unoriented simple closed curve $C \subset \Sigma$, we may associate to it $\pm h_L(C) \in \pm\mathbb{Z}^n$ by giving it an arbitrary orientation. One may imagine L as defining an abelian covering space of Σ, and then $\pm h_L(C)$ represents the absolute offset between the endpoints of C lifted to a path in that covering space.

Let $R_n = \mathbb{Z}[A^{\pm 1}][X_{\pm I} : I \in \mathbb{Z}^n \text{ and } I \neq 0]$; in the case all components of L are labeled by 1 (that is, if L is 1-*labeled*), then $R_1 = \mathbb{Z}[A^{\pm 1}, X_1, X_2, \dots]$. There is a ring homomorphism $\mathcal{H}(\Sigma) \to R_n$ given by $X_{\pm[C]} \mapsto X_{\pm h_L(C)}$, and with this we define a $\mathbb{Z}[A^{\pm 1}]$-linear map $\overline{h}_L : \mathrm{Sk}(\Sigma) \to R_n$ by considering the multiplicative factor of the skein's action on $\mathcal{H}$ and then mapping this to R_n. This has a state sum

given by

{eq:sk-map}
$$\overline{h}_L(S) = (-A^2 - A^{-2})^{b_0(S)} \prod_{C \in S} X_{\pm h_L(C)}, \tag{2.2}$$

where C ranges over the components of the simple skein S, and where $X_0 = 1$.

Definition 2.2. Given an oriented framed surface link L in a thickened surface $\Sigma \times I$ with components labeled from $\{1, 2, \ldots, n\}$, the *homological arrow polynomial* is $\mathcal{A}(L) = \overline{h}_L(L) \in R_n$.

If L is an unframed oriented surface link, then $(-A^3)^{-\mathrm{wr}(L)}\overline{h}_L(L)$ is the *normalized homological arrow polynomial*.

The following proposition is a special case of the fact that the homological arrow polynomial of a labeled oriented framed surface link determines the homological arrow polynomial of the link obtained by relabeling all of the components of a given label.

Proposition 2.3. *If L is a framed surface link with components labeled from $\{1, 2, \ldots, n\}$, then by taking $\mathcal{A}(L)$ and substituting $X_I = X_{\sum_i I_i}$ for each $I \in \mathbb{Z}^n$, the resulting polynomial in R_1 is the homological arrow polynomial for L with all components relabeled by 1.*

thm:h-evenness

Lemma 2.4. *For L a 1-labeled framed oriented surface link with a given framed diagram and for C a component of a state of L, then $h_L(C)$ is even.*

Proof. In the diagram for L, since L is oriented there is a well-defined right-handed pushoff, which can be thought of as being obtained by walking along the link in the link's orientation with one's right hand extended and tracing the path taken. Then, for the state curves, we will smooth the pushed-off version of L.

When smoothing a crossing, let us keep track of the local contribution to algebraic intersection number by drawing *whiskers*, which are small rays from L indicating the orientation of L where L intersects the state curves:

After orienting the state curves, the algebraic intersection number between L and a state curve C is the difference between the numbers of "left" whiskers and of "right" whiskers, from the point of view of someone taking a walk along C in the direction of its orientation. We can add an additional structure (similar to the "decorated magnetic virtual graphs" of [Miy08]) in the form of assigning orientations to each whisker-bound portion of the state curves:

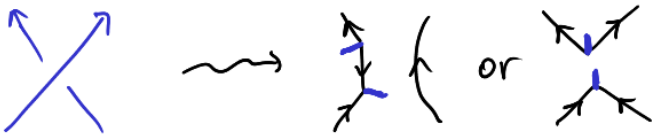

We immediately see each component of a state has an even number of whiskers due to the alternating arc orientations. □

Lemma 2.5. *The homological arrow polynomial is an invariant of framed virtual links.*

Proof. Consider a labeled framed oriented surface link L in $\Sigma \times I$, and suppose $\Sigma \subseteq \Sigma'$ for Σ' a compact oriented surface. The algebraic intersection numbers in Σ are the same as those in Σ', hence the homological arrow polynomials for L in $\Sigma \times I$ and in $\Sigma' \times I$ are the same. Hence, the polynomial is invariant under destabilization and therefore is a framed virtual link invariant. □

Remark 2.6. For computing the homological arrow polynomial of framed virtual links with components labeled from $\{1, 2, \dots, n\}$, the idea of whiskers from the proof of Lemma 2.4 can be modified by labeling each whisker by the label of the component of L that intersects there:

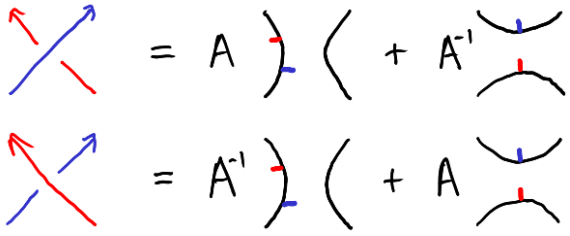

In the state sum's product, for a given component of the state, oriented arbitrarily, let m_i be the difference between the numbers of "left" whiskers and "right" whiskers of label i, and then one associates to that component the variable $X_{\pm(m_1,\dots,m_n)}$. For the $n = 1$ case, an algorithm for computing the arrow polynomial in this way (in consideration of Theorem 2.7) is given in Appendix A.

thm:arrow-poly-from-homol

Theorem 2.7. *Given a* 1*-labeled framed surface link* L*, then the Dye–Kauffman arrow polynomial and the homological arrow polynomial satisfy*

$$(-A^2 - A^{-2})\langle L\rangle_{\mathrm{A}} = \mathcal{A}(L)|_{X_i = K_{i/2} \text{ for all } i \geq 1},$$

where the division by two is justified by Lemma 2.4.

Proof. The Dye–Kauffman arrow polynomial is from expanding crossings according to Figure 2 then reducing cusps according to the following two rules:

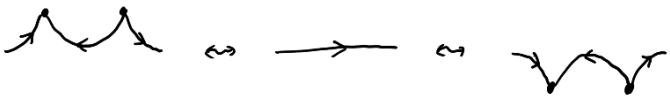

As a state sum,

$$\langle L\rangle_{\mathrm{A}} = \sum_S A^{a(S)-b(S)}(-A^2 - A^{-2})^{b_0(S)-1} \prod_{C \subseteq S} K_{\gamma(C)/2},$$

where $\gamma(C)$ is the number of cusps in component C after cusp reduction. This is an even number in consideration of the alternating arc orientations. After reduction, a component consists of a sequence of pairs of cusps of the following form:

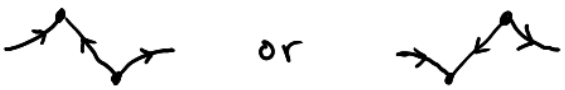

If we associate whiskers to cusps in the following manner,

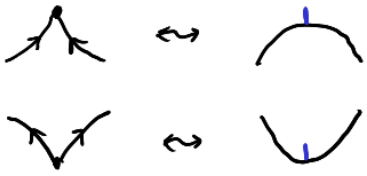

then we can see that the difference between "left" and "right" whiskers gives the total number of cusps after cusp reduction. This completes the verification. □

Example 2.8. The right-handed virtual Hopf link with components labeled by 1 and 2 has homological arrow polynomial $(-A^2 - A^{-2})(AX_{1,-1} + A^{-1}X_{1,1})$:

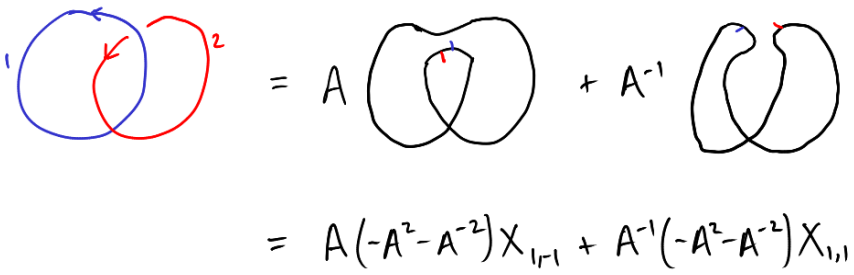

Hence, if each component is labeled by 1 the corresponding polynomial is $(-A^2 - A^{-2})(A + A^{-1}X_2)$ and thus the arrow polynomial is $A + A^{-1}K_1$.

3. Properties

sec:properties

3.1. Basic properties.

Proposition 3.1. *If L and L' are framed oriented virtual links each labeled from the same set $\{1, 2, \ldots, n\}$, then*

$$\mathcal{A}(L \sqcup L') = \mathcal{A}(L)\mathcal{A}(L').$$

A virtual link L is called a *connect sum* if there is a representative surface link $L \subset \Sigma \times I$ and a properly embedded annulus $A \subset \Sigma \times I$ that meets both components of $\Sigma \times \partial I$ such that A separates $\Sigma \times I$, A meets L transversely, and $|L \cap A| = 2$. A connect sum has a diagram D in a surface Σ such that there is a separating circle $C \subset \Sigma$ avoiding the crossings of D that intersects the arcs of D transversely in two points. This circle represents Σ as a connect sum $\Sigma_1 \# \Sigma_2$, and by cutting D apart along C, putting the respective pieces on Σ_1 and Σ_2, and connecting the endpoints of the cut arcs by trivial arcs, one obtains two surface link diagrams D_1 and D_2 in Σ_1 and Σ_2, respectively. If L_1 and L_2 are the respective corresponding virtual links, then we say $L = L_1 \# L_2$. While the connect sum of two oriented knots is a well-defined operation, this is not the case for virtual knots. The notation is only meant to signify that these three virtual links stand in this relation.

Proposition 3.2. *If L is a 1-labeled framed oriented virtual link that is a connect sum $L = L_1 \# L_2$, then*

$$(-A^2 - A^{-2})\mathcal{A}(L) = \mathcal{A}(L_1)\mathcal{A}(L_2).$$

thm:orientation-reversal

Proposition 3.3. *If L is a labeled framed oriented virtual link and $r_i L$ is L but with all components having label i given reversed orientation, then $\mathcal{A}(r_i L) = \mathcal{A}(L)|_{X_{\pm I} \mapsto X_{\pm r_i I}}$, where $r_i(m_1, \ldots, m_i, \ldots, m_n) = (m_1, \ldots, -m_i, \ldots, m_n)$.*

Proof. By reversing the orientation of all components of a particular label, in the state sum the whiskers of that label are all reflected over their respective component. Hence, the roles of "left" and "right" whiskers are reversed in the difference, so that label's count is negated. □

The following corollary is [DK09, Theorem 1.1].

Corollary 3.4. *If L is a 1-labeled framed virtual link, then $\mathcal{A}(L)$ is independent of the orientation of L.*

Proposition 3.5. *If L is a labeled framed oriented virtual link and L' is its mirror image, then*

$$\mathcal{A}(L) = \mathcal{A}(L')\big|_{A \mapsto A^{-1}}.$$

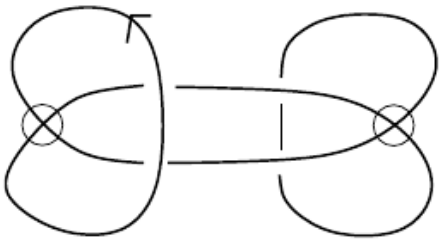

FIGURE 5. The virtual knot 4.55, known as *Kishino's knot*. fig:kishino

sec:genus-bounds

3.2. **Genus bounds.** For a labeled framed oriented surface link $L \in \Sigma \times I$, the homological arrow polynomial $\mathcal{A}(L)$ consists of terms of the form $pX_{\pm I_1} \cdots X_{\pm I_k}$ for $p \in \mathbb{Z}[A^{\pm 1}]$ and $I_i \in \mathbb{Z}^n$ nonzero for all $1 \le i \le k$, allowing duplicate factors. Each $X_{\pm I_i}$ comes from a loop in a state of the state sum, and since $I_i \neq 0$, it corresponds to a non-separating loop in Σ.

For homological reasons, if $\pm I_i \neq \pm I_j$, then the loops for I_i and I_j must not be isotopic. If the genus $g(\Sigma)$ is at most 1, then the maximum number of nonseparating pairwise non-isotopic disjoint loops is $g(\Sigma)$. For $g(\Sigma) \ge 2$, then a pants decomposition gives an upper bound of $3g(\Sigma) - 3$ of nonseparating pairwise non-isotopic disjoint loops. Thus, we may generalize the [DK09, Theorem 4.5] genus bound to use the homological arrow polynomial in the following theorem.

thm:genus-bound

Theorem 3.6. *Let $L \in \Sigma \times I$ be a labeled framed oriented surface link with Σ closed, and let $pX_{\pm I_1} \cdots X_{\pm I_k}$ be a term of $\mathcal{A}(L)$, where $p \in \mathbb{Z}[A^{\pm 1}]$ and $I_i \in \mathbb{Z}^n$ nonzero for all $1 \le i \le k$. If m is the number of pairwise distinct indices (that is, $m = |\{\pm I_i : 1 \le i \le k\}|$), then either (1) $g(\Sigma) \ge m$ if $g(\Sigma) \le 1$ or (2) $g(\Sigma) \ge \frac{1}{3}m + 1$ if $g(\Sigma) \ge 2$.*

thm:genus-bound-virt

Corollary 3.7. *Let m be the number of pairwise distinct indices in the $X_{\pm I}$ variables of a term of the homological arrow polynomial of a labeled framed oriented virtual link L. If m is 0 or 1, then m is a lower bound for the virtual genus of L. Otherwise, if $m \ge 2$, then $\lceil \frac{1}{3}m + 1 \rceil$ gives a lower bound for the virtual genus of L.*

Remark 3.8. Given any collection of nonseparating pairwise non-isotopic disjoint loops in a closed oriented surface, there exists an immersed loop whose algebraic intersection number with each of these loops is nonzero and even. Hence, we do not expect the $3g - 3$ bound to be improved except perhaps by considering the whole set of m numbers for every term in the homological arrow polynomial.

3.2.1. *Kishino's knot.* The virtual knot 4.55 (see Figure 5) is known to have a trivial Jones polynomial and a non-trivial arrow polynomial:

$$\langle K_{4.55} \rangle_{\mathrm{NA}} = A^4 + 1 + A^{-4} - (A^4 + 2 + A^{-4})K_1^2 + 2K_2.$$

By Corollary 3.7, we see the virtual genus of Kishino's knot is at least 1 (hence is definitely not a classical knot). The diagram for Kishino's knot can be drawn on a surface of genus 2. In Sections 3.5 and 4, we discuss the n-cabled arrow polynomial, which is the arrow polynomial of an n-cabling of a given virtual link. The n-cable of a virtual link has the same virtual genus. We

calculate the 2-cabled arrow polynomial of Kishino's knot to be, with the substitution $A = t^{-1/4}$,

$$\begin{aligned}
&-t^{9/2}+t^{7/2}+7t^{5/2}+15t^{3/2}+19t^{1/2}+19t^{-1/2}+15t^{-3/2}+7t^{-5/2}+t^{-7/2}-t^{-9/2}\\
&+K_4^2(-2t^{1/2}-2t^{-1/2})+K_3^2(-2t^{5/2}-4t^{3/2}-2t^{1/2}-2t^{-1/2}-4t^{-3/2}-2t^{-5/2})\\
&+K_2^2(t^{9/2}-t^{7/2}-6t^{5/2}-12t^{3/2}-14t^{1/2}-14t^{-1/2}-12t^{-3/2}-6t^{-5/2}-t^{-7/2}+t^{-9/2})\\
&+K_2^2K_4(2t^{5/2}+6t^{3/2}+8t^{1/2}+8t^{-1/2}+6t^{-3/2}+2t^{-5/2})\\
&+K_2^4(-t^{7/2}-4t^{5/2}-8t^{3/2}-11t^{1/2}-11t^{-1/2}-8t^{-3/2}-4t^{-5/2}-t^{-7/2})\\
&+K_1K_2K_3(2t^{7/2}+8t^{5/2}+20t^{3/2}+34t^{1/2}+34t^{-1/2}+20t^{-3/2}+8t^{-5/2}+2t^{-7/2})\\
&+K_1^2(-2t^{7/2}-8t^{5/2}-14t^{3/2}-16t^{1/2}-16t^{-1/2}-14t^{-3/2}-8t^{-5/2}-2t^{-7/2})\\
&+K_1^2K_2(4t^{7/2}+22t^{5/2}+50t^{3/2}+68t^{1/2}+68t^{-1/2}+50t^{-3/2}+22t^{-5/2}+4t^{-7/2})\\
&+K_1^2K_2^2(-2t^{7/2}-12t^{5/2}-32t^{3/2}-50t^{1/2}-50t^{-1/2}-32t^{-3/2}-12t^{-5/2}-2t^{-7/2})\\
&+K_1^4(-t^{7/2}-7t^{5/2}-21t^{3/2}-35t^{1/2}-35t^{-1/2}-21t^{-3/2}-7t^{-5/2}-t^{-7/2})
\end{aligned}$$

Since $K_1K_2K_3$ appears, we get the genus lower bound of $\frac{1}{3}\cdot 3+1=2$ for Kishino's knot. Therefore the virtual genus is exactly 2. This fact was previously shown in [DK], where they analyzed state curves of the Kauffman bracket expansion of Kishino's knot in a representative genus-2 surface.

sec:crossing-number

3.3. **Crossing number bounds.** The *crossing number* $c(L)$ of a surface link or virtual link L is the minimal number of crossings over all diagrams of the link. For a virtual link, the *virtual crossing number* $v(L)$ is the minimal number of virtual crossings over all planar immersions of diagrams of the virtual link.

The following proposition has not proved useful for determining the crossing number, since, except for the unknot, no virtual knot in Green's census gives an equality, and only 49 out of 2565 are only one off.

Proposition 3.9. *Let L be a surface link, and let $pX_{\pm I_1}\cdots X_{\pm I_k}$ be a term of $\mathcal{A}(L)$, where $p\in\mathbb{Z}[A^{\pm 1}]$ and $I_i\in\mathbb{Z}^n$ nonzero for all $1\le i\le k$. With $s=\sum_{i=1}^k\sum_{j=1}^n|I_{ij}|$, then $c(L)\ge\frac{1}{2}s$.*

Proof. Each crossing in the state sum introduces two whiskers. □

Corollary 3.10. *If $pK_{i_1}\cdots K_{i_k}$ is a term of the arrow polynomial $\langle L\rangle_{\mathrm{A}}$ of a virtual link L, where $p\in\mathbb{Z}[A^{\pm 1}]$ and $i_j\ge 1$ for all $1\le j\le k$, then $c(L)\ge\frac{1}{2}(i_1+\cdots+i_k)$.*

Conjecture 3.11. *If the breadth of $\mathcal{A}(L)$ as a polynomial in A is $4c(L)$, then the breadth of $\langle L\rangle$ is $4c(L)$.*

3.4. **Nullhomologous virtual links.**

Definition 3.12. For R a ring, an oriented surface link $L\subset\Sigma\times I$ is *R-nullhomologous* if $[L]=0$ in $H_1(\Sigma\times I;R)$. An oriented virtual link is *R-nullhomologous* if it has a representative surface link that is R-nullhomologous. We say a surface link or virtual link is *nullhomologous* if it is $\mathbb{Z}$-nullhomologous.

An important part of the theory of virtual links is Kuperberg's characterization, Theorem 3.13. For a thickened surface $\Sigma\times I$, a *vertical annulus* $A\subset\Sigma\times I$ is a properly embedded annulus that is isotopic to $C\times I$ for some simple closed curve $C\subset\Sigma$, and, for a given surface link $L\subset\Sigma\times I$, such an annulus is called *essential* if it does not bound a ball in $\Sigma\times I-L$. For a surface link $L\subset\Sigma\times I$ and a vertical annulus in the complement of A, there is a virtually equivalent surface link called the *destabilization of $L\subset\Sigma\times I$ along A*, described as follows. After an ambient isotopy we may assume $A=C\times I$, and, with $\nu(C)$ being a tubular neighborhood of C in Σ such that $\nu(C)\times I$ is disjoint from L, then $L\subset(\Sigma-\nu(C))\times I$ is a virtually equivalent surface link. Capping off each component

of $\partial(\Sigma - \nu(C))$ with a disk yields a closed surface Σ', and $L \subset \Sigma' \times I$ is the destabilization of $L \subset \Sigma \times I$ along A.

A *spanning* surface link $L \subset \Sigma \times I$ is one where L meets each component of $\Sigma \times I$.

thm:what-is-virtual-link

Theorem 3.13 ([Kup03])**.** *Given a virtual link L, there is a representative spanning surface link $L \subset \Sigma \times I$ with Σ closed such that every vertical annulus in $\Sigma \times I - L$ bounds a ball disjoint from L. This surface link is unique up to both isotopy and transformations induced by orientation-preserving self-diffeomorphisms of Σ.*

Proof sketch. Given a disjoint union $\mathcal{A}$ of vertical annuli in $\Sigma \times I - L$, let the *pruned destabilization along $\mathcal{A}$ of $L \subset \Sigma \times I$* be the result of destabilizing $L \subset \Sigma \times I$ along all the annuli in $\mathcal{A}$ and then throwing away every component of the resulting thickened surface that does not meet L, yielding a spanning surface link that is virtually equivalent to $L \subset \Sigma \times L$. An *irreducible descendant* of $L \subset \Sigma \times I$ is a pruned destabilization where every vertical annulus in the complement of L bounds a ball disjoint from L. If there were a spanning surface link with multiple non-diffeomorphic irreducible descendants, we could let $L \subset \Sigma \times I$ be one with $g(\Sigma) - b_0(\Sigma) + b_0(L) \in \mathbb{N}$ minimal. Thus, the destabilization along any essential vertical annulus for this surface link has a unique irreducible descendant.

The way the proof proceeds is to suppose there are nonempty disjoint unions $\mathcal{A}_1$ and $\mathcal{A}_2$ of essential vertical annuli in $\Sigma \times I$ whose pruned destabilizations have non-diffeomorphic irreducible descendants that, when put in general position, intersect in the fewest number of curves. The intersection is analyzed to show that either $g(\Sigma) - b_0(\Sigma) + b_0(L)$ was not minimal or that either $\mathcal{A}_1$ or $\mathcal{A}_2$ can be modified to have fewer components in the intersection without changing the diffeomorphism class of its irreducible descendent.

Therefore, there is a unique irreducible descedant for every surface link and hence for each virtual equivalence class. □

Proposition 3.14. *If L is an R-nullhomologous oriented virtual link and $L \subset \Sigma \times I$ is a genus-minimal representative surface link with Σ closed, then the surface link is R-nullhomologous.*

Proof. Let $L \subset \Sigma \times I$ be a spanning surface link with Σ. If this is not the unique representative from Theorem 3.13, then after an isotopy there is a finite collection $\mathcal{C} = C_1 \sqcup C_2 \sqcup \cdots \sqcup C_n \subset \Sigma$ of disjoint simple closed curve such that the pruned destabilization along $\mathcal{A} = \mathcal{C} \times I$ gives the unique representative $L \subset \Sigma' \times I$.

Supposing $L \subset \Sigma \times I$ is R-nullhomologous, there is some nonzero $n \in \mathbb{Z}$ such that $n[L] = 0$ in $H_1(\Sigma \times I; \mathbb{Z})$. Hence, there is a 2-chain $S \in C_2(\Sigma \times I; \mathbb{Z})$ with $\partial S = nL$ that, outside a regular neighborhood of L, is an oriented embedded surface. We may assume S intersects $\mathcal{A}$ transversely in a collection of simple closed curves. Considering $S - \nu(\mathcal{C}) \subset \Sigma' \times I$, we may cap off the newly formed boundary $S \cap \mathrm{cl}(\nu(\mathcal{C}))$ with disks in the capped-off region of $\Sigma' \times I$, forming $S' \subset \Sigma' \times I$ which, outside a regular neighborhood of L, is an oriented embedded surface. Thus, $n[L] = 0$ in $H_1(\Sigma' \times I; \mathbb{Z})$, and therefore $L \subset \Sigma' \times I$ is R-nullhomologous. □

Remark 3.15. It is not true that every representative surface link of an R-nullhomologous virtual link is R-nullhomologous. For example, consider a homologically nontrivial simple closed curve C in a closed oriented surface Σ.

Proposition 3.16. *If $L = L_1 \sqcup \cdots \sqcup L_n$ is a labeled framed oriented virtual link with each L_i nullhomologous, then $\mathcal{A}(L) \in \mathbb{Z}[A^{\pm 1}]$.*

Proof. Since each L_i is nullhomologous, the function h_L is the constant-zero function, hence only $X_0 = 1$ appears in the state sum. □

The following is a restatement of [DK09, Theorem 1.5] and [Miy08, Proposition 5.8] in terms of the homological arrow polynomial.

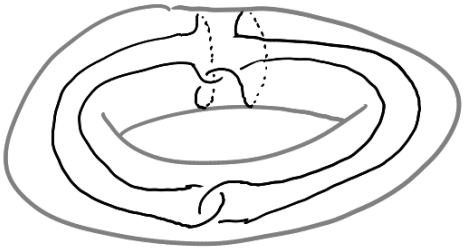

FIGURE 6. The virtual knot 4.105, drawn on a torus so that it is obviously nullhomologous. fig:4n105

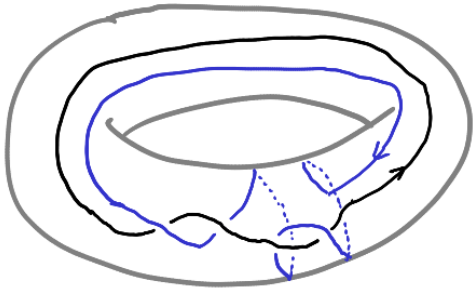

FIGURE 7. A nullhomologous virtual link. fig:vlink1

Corollary 3.17. *If L is a classical link (that is, a surface link in $S^2 \times I$), then*

$$\mathcal{A}(L) = (-A^2 - A^{-2})\langle L \rangle,$$

where $\langle L \rangle$ is the Kauffman bracket.

Proof. $H_1(S^2 \times I; \mathbb{Z}) = 0$. □

Example 3.18. The virtual knot 4.105 has virtual genus 1 and is nullhomologous (see Figure 6), hence we expect $\mathcal{A}(K_{4.105}) \in \mathbb{Z}[A^{\pm 1}]$. Indeed:

$$\mathcal{A}(K_{4.105}) = (-A^2 - A^{-2})(A^8 + 1 - A^{-4}).$$

Example 3.19. The virtual link L in Figure 7, with the black component labeled by 1 and the blue component labeled by 2 has

$$\mathcal{A}(L) = (-A^2 - A^{-2})\left(-A^6 + A^2 - 2A^{-2} + (-A^2 + A^{-2} + A^{-6} - A^{-10})X_{1,-1}^2\right).$$

We can see how its arrow polynomial is in $\mathbb{Z}[A^{\pm 1}]$ since $X_{1,-1} \mapsto X_0$ when relabeling the components by 1. Thus, the homological arrow polynomial can sometimes detect non-classicality where the arrow polynomial cannot. However, if we reverse the orientation of the blue component, the corresponding arrow polynomial is

$$\langle L \rangle_{\mathrm{A}} = -A^6 + A^2 - 2A^{-2} + (-A^2 + A^{-2} + A^{-6} - A^{-10})K_1^2,$$

so the set of arrow polynomials of all orientations of the link components is able to detect non-classicality.

Passing to $\mathbb{Z}/m\mathbb{Z}$ coefficients with the algebraic intersection numbers, one obtains polynomials $\mathcal{A}_{\mathbb{Z}/m\mathbb{Z}}(L) \in \mathbb{Z}[A^{\pm 1}][X_{\pm I} : I \in (\mathbb{Z}/m\mathbb{Z})^n \text{ and } I \neq 0]$, which can be obtained by reducing the indices of each $X_{\pm I}$ in $\mathcal{A}(L)$ modulo m, setting $X_0 = 1$. If L is $\mathbb{Z}/m\mathbb{Z}$ nullhomologous, then $\mathcal{A}_{\mathbb{Z}/m\mathbb{Z}}(L) \in \mathbb{Z}[A^{\pm 1}]$. In consideration of Lemma 2.4, this gives nothing for $\mathbb{Z}/2\mathbb{Z}$-nullhomologous links (and, in fact,

$\mathcal{A}_{\mathbb{Z}/2\mathbb{Z}}(L) = \langle A \rangle$ if L is 1-labeled), however, for other moduli we can restrict the ring for $\mathcal{A}(L)$ as in the following proposition.

Proposition 3.20. *If L is a 1-labeled $\mathbb{Z}/m\mathbb{Z}$-nullhomologous virtual link, then*

$$\mathcal{A}(L) \in \mathbb{Z}[A^{\pm 1}, X_m, X_{2m}, X_{3m}, \dots].$$

If m is odd, then $\mathcal{A}(L) \in \mathbb{Z}[A^{\pm 1}, X_{2m}, X_{4m}, X_{6m}, \dots]$.

sec:checkerboard

3.5. **Checkerboard colorability.** A virtual link L is checkerboard colorable (introduced in [Kam02]) if it has a surface link representative $L \subset \Sigma \times I$ such that the diagram for L in that surface is checkerboard colorable. As the following proposition shows, a virtual link is checkerboard colorable if and only if it is $\mathbb{Z}/2\mathbb{Z}$-nullhomologous.

thm:checkerboard-z2

Proposition 3.21 ([BK, Proposition 1.7])**.** *For a surface link $L \subset \Sigma \times I$, the following are equivalent:*

1. *The link is checkerboard colorable.*
2. *The link is the boundary of an unoriented spanning surface $F \subset \Sigma \times I$.*
3. *The link is $\mathbb{Z}/2\mathbb{Z}$-nullhomologous.*

Proof. That (2) implies (3) is that F can be thought of as a 2-chain with $\mathbb{Z}/2\mathbb{Z}$ coefficients, and the converse is the standard construction of a spanning surface from a simplicial 2-chain with $\mathbb{Z}/2\mathbb{Z}$ coefficients.

The equivalence of (2) and (3) is from noting that $\Sigma \times I$ deformation retracts onto Σ. Put L into a position where the projection to Σ is transverse with transverse double points, and let $C \subset \Sigma$ be the projection. If L is checkerboard colorable — that is, if the regions outside C can be checkerboard colored — then the black regions of the coloring form a 2-chain in $C_2(\Sigma; \mathbb{Z}/2\mathbb{Z})$ whose boundary is C as an element of $C_1(\Sigma; \mathbb{Z}/2\mathbb{Z})$. Conversely, if $[C] = 0$ in $H_1(\Sigma; \mathbb{Z}/2\mathbb{Z})$, then there is a simplicial 2-chain in $C_2(\Sigma; \mathbb{Z}/2\mathbb{Z})$ whose boundary is C, and the checkerboard coloring comes from the coefficients of the 2-simplicies. □

One class of checkerboard colorable virtual links are those that are alternating.

Proposition 3.22 ([Kam02, Lemma 7])**.** *If L is an alternating virtual link, then it is checkerboard colorable.*

Proof. Consider a diagram D for L on a closed oriented surface Σ such that each region of $\Sigma - D$ is a disk. For example, Σ could be the surface from Theorem 3.13. By performing the A smoothing of each crossing, one obtains a closed 1-manifold S, which, due to D being alternating, we may assume lies in the boundary of a regular neighborhood of D. Hence, each component of S bounds a disk and is thus nullhomologous. As S is $\mathbb{Z}/2\mathbb{Z}$-homologous to L, it follows from Proposition 3.21 that L is checkerboard colorable. □

As a quick corollary, by using idea of the proof we get the following result for *positive* virtual links, which are virtual links where every crossing is positive.

Corollary 3.23. *If L is a positive alternating virtual link, then it is $\mathbb{Z}$-nullhomologous, and therefore $\mathcal{A}(L) \in \mathbb{Z}[t^{\pm 1}]$.*

An interesting fact about having a checkerboard coloring is that the state loops can be canonically oriented. The coloring induces a coloring of the regions in the complement of a given state, and the state loops are the oriented boundary of the resulting black region:

Hence, a framed oriented virtual link L with a fixed checkerboard coloring C does not have a sign ambiguity in the algebraic intersection numbers, and so we may define a polynomial $\mathcal{A}(L,C) \in \mathbb{Z}[A^{\pm 1}][X_I : I \in \mathbb{Z}^n \text{ and } I \neq 0]$. One has $\mathcal{A}(L) = \mathcal{A}(L,C)|_{X_I \mapsto X_{\pm I}}$.

Suppose L is 1-labeled and consider the whiskers in the expansion for $\mathcal{A}(L)$. The whiskers come in pairs, where evidently one points into the black region and the other points into the white region. Hence, if we interpret the whiskers as vectors inducing a flow across the state circles between the white and black regions, the total flow into the black region is 0. Thus, if $pX_{i_1}X_{i_2}\cdots X_{i_k}$ is a term of $\mathcal{A}(L,C)$ with $p \in \mathbb{Z}[A^{\pm 1}]$ and $i_j \in \mathbb{Z} - \{0\}$ for each $1 \leq j \leq k$, allowing duplicates, then $\sum_{j=1}^{k} i_j = 0$. Since $i_k = -\sum_{j=1}^{k-1} i_j$, the triangle inequality yields

$$|i_k| = \left|\sum_{j=1}^{k-1} i_j\right| \leq \sum_{j=1}^{k-1} |i_j|.$$

Furthermore, Lemma 2.4 implies $|i_j|$ is even for all j. Summarizing, we have reproved:

thm:deng2020

Theorem 3.24 ([DJK, Theorem 4.3])**.** *Let L be a checkerboard colorable 1-labeled oriented framed virtual link. Then, for each term $pX_{i_1}X_{i_2}\cdots X_{i_k}$ of $\mathcal{A}(L)$ with $p \in \mathbb{Z}[A^{\pm 1}]$ and $i_j \geq 1$ for all $1 \leq j \leq k$, allowing duplicate factors,*

(1) $\sum_{j=1}^{k} i_j \equiv 0 \pmod 4$, *and*
(2) $i_k \leq \sum_{j=1}^{k-1} i_j$.

In particular, $k \geq 2$.

In [DJK], they use this theorem to resolve checkerboard non-colorability of six of the seven exceptions from [Ima16], which are 4.55, 4.56, 4.59, 4.72, 4.76, 4.77, 4.96, where the theorem says nothing about 4.72 since $\mathcal{A}(K_{4.72}) = 1$. In all cases, the condition that $k \geq 2$ for each term suffices.

We resolve the case of 4.72 by using cabled arrow polynomials. Given a framed surface link, recall that the n-cabling is the framed surface link obtained from embedding n parallel annuli along the link's framing annulus. In the case of a $(2k+1)$-cabling, checkerboard colorability is preserved. For example,

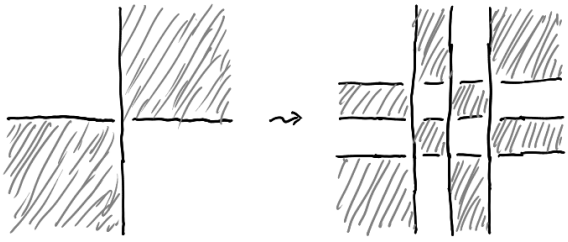

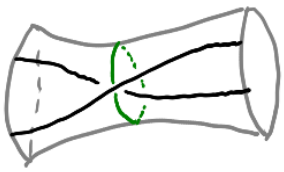

FIGURE 8. A non-reduced surface link diagram contains a separating loop (green) intersecting the knot through a single crossing. fig:non-reduced

The homological arrow polynomial of the 3-cabling of the 0-framed 4.72, with the substitution $A = t^{-1/4}$, is

$$\begin{aligned}
&-2t^8+4t^7+29t^6+108t^5+273t^4+575t^3+952t^2+1298t+1426+1298t^{-1}\\
&+952t^{-2}+575t^{-3}+273t^{-4}+108t^{-5}+29t^{-6}+4t^{-7}-2t^{-8}\\
&+X_{18}(t^{13/2}+4t^{11/2}+17t^{9/2}+44t^{7/2}+80t^{5/2}+108t^{3/2}+121t^{1/2}+121t^{-1/2}\\
&+108t^{-3/2}+80t^{-5/2}+44t^{-7/2}+17t^{-9/2}+4t^{-11/2}+t^{-13/2})\\
&+X_{12}(8t^7+44t^6+142t^5+328t^4+618t^3+944t^2+1210t+1308+1210t^{-1}\\
&+944t^{-2}+618t^{-3}+328t^{-4}+142t^{-5}+44t^{-6}+8t^{-7})\\
&+X_6(-8t^{15/2}-28t^{13/2}-69t^{11/2}-116t^{9/2}-130t^{7/2}-41t^{5/2}+111t^{3/2}+242t^{1/2}+242t^{-1/2}\\
&+111t^{-3/2}-41t^{-5/2}-130t^{-7/2}-116t^{-9/2}-69t^{-11/2}-28t^{-13/2}-8t^{-15/2})\\
&+X_6X_{12}(-10t^{13/2}-39t^{11/2}-88t^{9/2}-148t^{7/2}-219t^{5/2}-300t^{3/2}-360t^{1/2}-360t^{-1/2}\\
&-300t^{-3/2}-219t^{-5/2}-148t^{-7/2}-88t^{-9/2}-39t^{-11/2}-10t^{-13/2})\\
&+X_6^2(2t^9-24t^7-115t^6-327t^5-709t^4-1252t^3-1857t^2-2347t-2534-2347t^{-1}\\
&-1857t^{-2}-1252t^{-3}-709t^{-4}-327t^{-5}-115t^{-6}-24t^{-7}+2t^{-9})\\
&+X_6^3(4t^{15/2}+18t^{13/2}+44t^{11/2}+82t^{9/2}+126t^{7/2}+165t^{5/2}+190t^{3/2}+199t^{1/2}+199t^{-1/2}\\
&+190t^{-3/2}+165t^{-5/2}+126t^{-7/2}+82t^{-9/2}+44t^{-11/2}+18t^{-13/2}+4t^{-15/2})
\end{aligned}$$

We notice, for instance, X_{12} by itself, thus the $k \geq 2$ condition of Theorem 3.24 implies the 3-cabling of 4.72 is not checkerboard colorable, and therefore 4.72 is not checkerboard colorable.

This completes Imabeppu's characterization of checkerboard colorability of all virtual knots up to four crossings.

3.6. **Alternating virtual links.** For classical links, a *reduced* alternating link diagram is one with no nugatory crossings. That is, the identities of the opposite regions at each crossing are distinct. Since link diagrams are checkerboard colorable, this implies that the identities of all four regions around a crossing are distinct. Kamada in [Kam] calls a virtual link diagram *proper* if, when it is cellularly embedded, the identities of all four regions are distinct around each crossing. The Kauffman–Murasugi–Thistlethwaite theorem says that a connected reduced alternating link diagram D satisfies $\text{breadth}\langle D\rangle = 4c(D)$. Kamada shows that if D is a connected proper alternating virtual link diagram, then $\text{breadth}\langle D\rangle = 4(c(D) - g(D))$.

A generalization of this result is in [BK], where they define a *reduced* surface link diagram to be one that is cellularly embedded where there are no separating simple closed curve in the surface that intersect the diagram through a single crossing like in Figure 8. Equivalently, a cellularly embedded surface link diagram is reduced if, whenever the two regions opposite a crossing are identical, then removing the interior of that region and a neighborhood of the crossing does not disconnect the surface. They introduce homological information to the Kauffman bracket to form

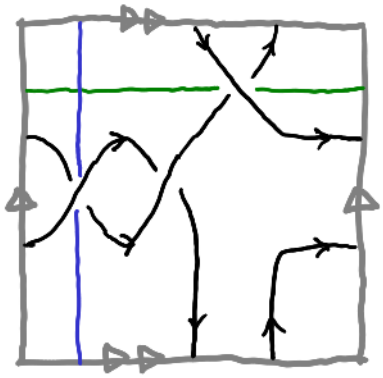

FIGURE 9. A reduced diagram of 3.7 on a torus. The green loop shows the virtual knot is not h-reduced, and both the green and blue loops show it is not proper. fig:3.7-loops

the *homological Kauffman bracket*, with which they prove two of the Tait conjectures generalized to virtual links: if D_1 and D_2 are two reduced connected alternating virtual link diagrams for the same virtual link L, then $c(D_1) = c(D_2) = c(L)$ and $\mathrm{wr}(D_1) = \mathrm{wr}(D_2)$.

As a curiosity, we prove an analogue of the Kauffman–Murasugi–Thistlethwaite theorem using the arrow polynomial. A labeled surface link diagram is *h-reduced* if every simple closed curve C in the surface that passes through a single crossing has nonzero algebraic intersection number with each component of the link. The blue loop in Figure 9 is allowed in an h-reduced diagram, but the green loop is not. Every proper diagram is h-reduced, and every h-reduced cellularly embedded diagram is reduced.

Let $\mathcal{A}'(L)$ be the result of substituting $X_I \mapsto X_I(-A^2 - A^{-2})^{-1}$ for each index I, which gives another element of R_n. Considering a nonzero $p \in R_n$ as a polynomial in A, let $\mathrm{maxdeg}_A p$ and $\mathrm{mindeg}_A p$ respectively denote the maximum and minimum degrees of A in terms of p, and let $\mathrm{breadth}_A p = \mathrm{maxdeg}_A p - \mathrm{mindeg}_A p$.

Definition 3.25. Let D be a labeled virtual link diagram for a labeled virtual link L, and for a state S of D, let $i(S)$ be the number of loops $C \subseteq S$ such that $h_L(C) = 0$ (the number of "inessential" state loops). The diagram D is called *A-h-adequate* if for every state S' with $b(S') = 1$, then $i(S') \le i(S_A)$. Similarly, D is called *B-h-adequate* if for every state S' with $a(S') = 1$, then $i(S') \le i(S_B)$. If D is both A-h-adequate and B-h-adequate, then D is called *h-adequate*.

Proposition 3.26. *Let D be an h-reduced labeled alternating virtual diagram. Then D is h-adequate.*

Proof. After cellularly embedding the diagram, the A-state S_A consists of simple closed curves that bound disks in the surface since the diagram is alternating. For any checkerboard colored diagram, the state loops can be put in a form where, away from crossings, the diagram is disjoint from the black regions, and near crossings whiskers only appear when the crossing is contained in the black region:

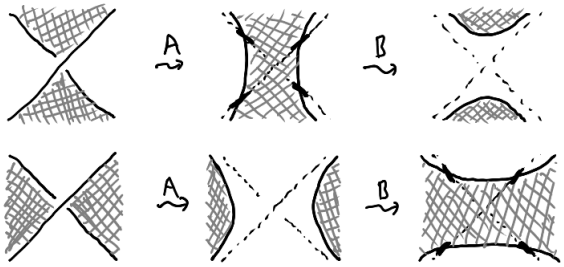

The whiskers, here, are illustrated ambiguously, and their orientation depends on the orientation of the link. For the checkerboard coloring of the alternating diagram, we may assume the S_A loops bound black disks, and every black disk is disjoint from the crossings, hence there are no whiskers. Since each loop is nullhomotopic, $i(S_A) = b_0(S_A)$.

Let S' be a state with $b(S') = 1$, and let c refer to the B-smoothed crossing. This introduces four whiskers, and, by consideration of the checkerboard coloring, either two state loops merge into one, or one state loop splits into two. In the case where two state loops merge into one, then $b_0(S') = b_0(S_A) - 1$ and the resulting loop C might have $h_L(C) \neq 0$, so $i(S') \leq i(S_A)$. In the case where a state loop splits, then $b_0(S') = b_0(S_A) + 1$ and there is a black disk that, together with a neighborhood of c, contains an essential loop:

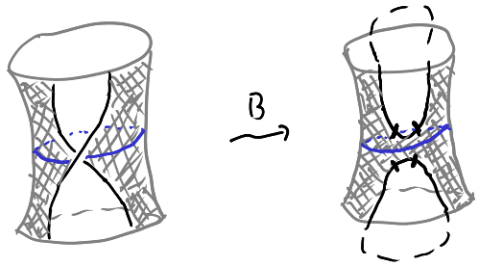

In the B-smoothed version, which is S', by the assumption that the link is h-reduced, all four whiskers are either pointing up or pointing down. Thus, they both have nonzero algebraic intersection number with each component of the link, hence $i(S') = i(S_A)$.

Therefore, the diagram is A-h-adequate. By a similar argument, the diagram is also B-h-adequate, and thus h-adequate. □

Proposition 3.27. *Let D be an h-adequate labeled virtual link diagram for a virtual link L. Then* $\mathrm{breadth}_A(\mathcal{A}'(L)) = 2c(D) + 2i(S_A) + 2i(S_B)$.

Proof. By the usual argument, if D is A-h-adequate then nothing cancels out the A-state's contribution to $\mathrm{maxdeg}_A(\mathcal{A}'(L))$ and the B-state's contribution to $\mathrm{mindeg}_A(\mathcal{A}'(L))$. The maximal A-degree from the term for the A-state S_A is $a(S_A) - b(S_A) + 2i(S_A) = c(D) + 2i(S_A)$. Similarly, the minimal A-degree of the term for the B-state S_B is $a(S_B) - b(S_B) - 2i(S_B) = -c(D) - 2i(S_B)$. Hence, $\mathrm{breadth}_A(\mathcal{A}'(L)) = 2c(D) + 2i(S_A) + 2i(S_B)$. □

Corollary 3.28. *Let D be an h-reduced connected alternating labeled virtual diagram for a virtual link L. Then* $\mathrm{breadth}_A(\mathcal{A}'(L)) = 4c(D) - 4g(D)$, *where $g(D)$ is the genus of the surface D cellularly embeds into.*

Proof. Since $i(S_A)$ is the number of black disks and $i(S_B)$ is the number of black disks when the diagram is cellularly embedded in a connected surface Σ, by Euler characteristics for the disks and the diagram as a cellular decomposition of Σ we have $c(D) - 2c(D) + (i(S_A) + i(S_B)) = 2 - 2g(\Sigma)$. □

4. Computational investigations

sec:computational-investigations

We implemented the arrow polynomial in Virtual KnotFolio [Mil20] for the purpose of better identifying knots. We also implemented the *n-cabled arrow polynomial*, which is the arrow polynomial of the n-cabling of the 0-framing of a given oriented virtual link, and, so that it it more easily relates to the Jones polynomial, we substitute $A = t^{-1/4}$. The algorithm is essentially the one listed in Appendix A, which is to use a "virtual Temperley–Lieb planar algebra" that has been augmented with whiskers. The planar algebra has the property that virtual tangles may be reduced to a normal form. We also use the frontier-minimization heuristic to decide on the order in which crossings are joined to the developing tangle.

TABLE 1. Virtual knots up to four crossings with non-unique arrow polynomials. Each row consists of virtual knots with the same arrow polynomial.

tab:arrow-non-unique

0.1	4.46	4.72	4.98	4.107
2.1	4.33	4.44		
3.2	4.27			
3.6	4.105			
3.7	4.85	4.96	4.106	
4.1	4.7			
4.11	4.63			
4.13	4.55	4.56		
4.15	4.29			
4.16	4.68			
4.2	4.8	4.51	4.71	
4.20	4.34			
4.25	4.43			
4.38	4.49			
4.4	4.5	4.18	4.30	
4.40	4.52			
4.45	4.83			
4.47	4.97			
4.50	4.70			
4.58	4.75			
4.59	4.76	4.77		
4.9	4.61			
4.99	4.108			

The cabled arrow polynomials stand in relation to the *colored arrow polynomials* in the same way that the cabled Jones polynomials do to the colored Jones polynomials. For the nth colored arrow polynomial, we would form the n-cabling and then splice in the nth Jones–Wenzl projector into each component. The first n cabled arrow polynomials determine the first n colored arrow polynomials, and vice versa.

While the arrow polynomial by itself is able to distinguish the 117 virtual knots in Green's census up to four crossings except for the 58 in Table 1, the first and second cabled arrow polynomials together fully determine the virtual knot. In contrast, the first and second cabled Jones polynomials are unable to distinguish the virtual knots listed in Table 2.

For the 2565 virtual knots in Green's census up to five crossings, all the virtual knots are able to be distinguished by the first and second cabled arrow polynomials except for the 18 listed in Table 3. The Alexander polynomial is able to distinguish the last four pairs in this table, hence there are only five undistinguished pairs.

We have not explored taking advantage of the fact that an n-cabling is a link, so we may compute the homological arrow polynomial. This might potentially allow the remaining pairs to be distinguished.

5. MISCELLANEOUS

5.1. **Mutation.** For a surface link $L \subseteq \Sigma \times I$, a *Conway annulus* is a vertical annulus $A \subset \Sigma \times I$ that separates $\Sigma \times I$ such that A intersects L transversely in exactly four points. This corresponds to a separating circle in Σ that intersects the diagram for L in exactly four points.

TABLE 2. Virtual knots up to four crossings with non-unique first and second cabled Jones polynomials. Each row consists of virtual knots with the same such polynomials.

tab:jones-non-unique

0.1	4.55	4.56	4.76	4.77
2.1	4.4	4.5	4.54	4.74
3.3	4.63			
4.1	4.3	4.7	4.53	4.73
4.13	4.59	4.107		
4.19	4.42			
4.2	4.6	4.8	4.12	4.75
4.26	4.97			
4.28	4.83			
4.95	4.101			

TABLE 3. Virtual knots up to five crossings with non-unique first and second arrow polynomials. Each row consists of pair of virtual knots with the same such polynomials.

tab:cabled-arrow-non-unique

5.196	5.1662
5.197	5.1657
5.204	5.1670
5.205	5.1665
5.2322	5.2411
5.287	5.1168
5.294	5.1175
5.295	5.1176
5.302	5.1183

Like the usual Conway mutation, we may cut along A, flip one piece of $\Sigma \times I$ over in a way that swaps the points of $L \cap A$ in pairs, and then reglue. For example,

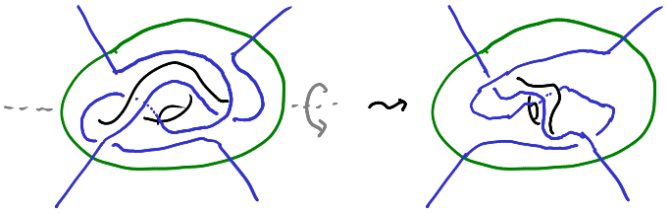

For a virtual link diagram in the plane, this mutation operation does correspond to finding a Conway circle that intersects the virtual link in four points.

The arrow polynomial is not invariant under mutation. For example, the mutant virtual knots in Figure 10 (from [FK]) have

$$W(K_{3.2}) = t^2 - t + 1 + (-t^{1/2} + t^{-1/2})K_1$$
$$W(K_{5.632}) = -t + 1 - tK_4 + (t^2 + t)K_2^2 + (-t^{1/2} + t^{-1/2})K_1.$$

As expected, substituting $K_i = 1$ for all i gives identical Jones polynomials.

However, the arrow polynomial is invariant under certain types of mutations.

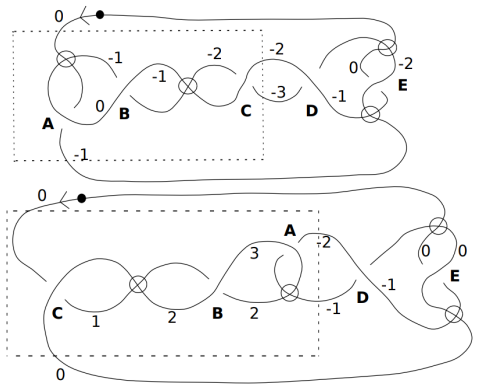

FIGURE 10. Mutant virtual knots (3.2 and 5.632) with different arrow polynomials. fig:mutants

Proposition 5.1. *Let C be a Conway circle for a diagram of a surface link L in Σ, and let Σ_1 and Σ_2 be the closures of the two pieces of $\Sigma - C$. If L is homologous to a multicurve $\lambda \subset \Sigma_1$, then the arrow polynomial for L is invariant under every mutation with respect to C. This is the case, in particular, if C bounds a disk in Σ.*

Proof. Since L is homologous to a multicurve λ in Σ_1, then the algebraic intersection numbers can be calculated with respect to λ instead of the projection of L. Hence, in every state, we may assume there are no whiskers in the Σ_2 side. After evaluating loops in the Σ_2 side, there are only three cases for the state curves in Σ_2, and they all remain invariant under mutation. □

Corollary 5.2. *If C is a Conway circle for a virtual link diagram of a link L such that one side of C contains no virtual crossings, then the arrow polynomial for L is invariant under mutations with respect to C.*

ACKNOWLEDGEMENTS

I would like to thank Louis Kauffman for suggesting I implement the arrow polynomial in Virtual KnotFolio [Mil20] and for helpfully sharing Mathematica code with me, Allison Henrich for some discussion about virtual knots and encouraging me to write this paper, and Ian Agol for his usual helpful advice.

APPENDIX A. COMPUTING THE ARROW POLYNOMIAL

sec:computing-arrow

The following is a Mathematica program for computing the (unnormalized) arrow polynomial of a virtual link given in oriented PD format. Following the convention of the `KnotTheory`` Mathematica package, oriented crossings are represented by `Xp` and `Xm` forms as follows:

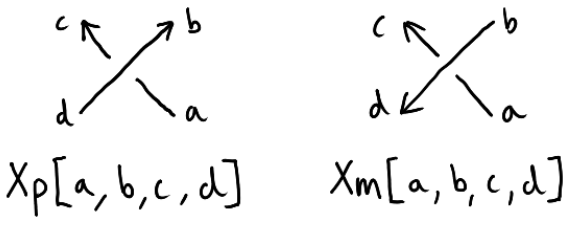

The rules in `arrowRules` give the expansion of oriented crossings with whiskers as described in Lemma 2.4. The `arrow` function cuts open the virtual link to form a 1-1 tangle since this saves having to divide by $-A^2 - A^{-2}$ in the end.

```
ClearAll[whiskers, K, arrow];

(* K[n] corresponds to the variable K_n *)
K[0] = 1;

(* whiskers[n, a, b] represents a path from arc id a to arc id b with
   n whiskers to the left if n is positive, and -n whiskers to the right
   if n is negative *)

whiskers /: whiskers[n_, a_, b_] whiskers[m_, b_, c_] := whiskers[n + m, a, c];
whiskers /: whiskers[n_, a_, b_] whiskers[m_, c_, b_] := whiskers[n - m, a, c];
whiskers /: whiskers[n_, a_, b_] whiskers[m_, a_, c_] := whiskers[n - m, c, b];
whiskers /: x_whiskers^2 := x x;
whiskers[n_, a_, a_] := (-A^2 - A^-2) K[Abs[n]/2];
whiskers[n_, a_, b_] /; b < a := whiskers[-n, b, a]; (* a normalization *)

arrowRules = {
  Xp[a_, b_, c_, d_] :>
    A whiskers[0, a, b] whiskers[0, c, d]
    + A^-1 whiskers[-1, a, d] whiskers[1, c, b],
  Xm[a_, b_, c_, d_] :>
    A^-1 whiskers[0, b, c] whiskers[0, d, a]
    + A whiskers[-1, b, a] whiskers[1, d, c]
 };

arrow[pd_PD] := With[{max = Max[List @@@ (List @@ pd)]},
  With[{newpd = ReplacePart[pd, FirstPosition[pd, max] -> max + 1]},
    (* Now newpd is a 1-1 tangle *)
    With[{exp = Expand[Times @@ (newpd /. arrowRules)] /.
                  whiskers[n_, max, max + 1] :> K[Abs[n]/2]
        },
      exp // Collect[#, A, Simplify] &]]];
```

For example,

```
(* 2.1 - Virtual trefoil *)
In[1]:= green2n1 = PD[Xm[1, 2, 3, 4], Xm[4, 3, 1, 2]];
In[2]:= arrow[green2n1]
Out[2]= 1/A^2 + K[1] - A^4 K[1]

(* 3.7 - Virtualized trefoil *)
In[3]:= green3n7 = PD[Xm[2, 5, 1, 4], Xp[4, 6, 3, 1], Xp[6, 2, 5, 3]];
In[4]:= arrow[green3n7]
Out[4]= -A^3 K[1]^2 + (-1 + K[1]^2)/A^5

(* Virtual Hopf link *)
In[5]:= vhopf = PD[Xm[1, 2, 1, 2]];
In[6]:= arrow[vhopf]
Out[6]= 1/A + A K[1]

(* 4.105 *)
In[7]:= green4n105 = PD[Xp[8, 4, 7, 5], Xp[4, 8, 3, 1],
                        Xp[2, 6, 1, 7], Xp[6, 2, 5, 3]];
In[7]:= arrow[green4n105]
Out[7]= 1 - 1/A^4 + A^8
```

Appendix B. Computing the homological arrow polynomial

The following Mathematica program computes the homological arrow polynomial $\mathcal{A}(L)$ of a virtual link L given in oriented PD format using the harrow function. The component labeling is given by the arc id modulo 10, and it is up to the user to verify that all arc ids in a given component are the same modulo 10.

```
(* X[i1,i2,...] represents X_{\pm(i1,i2,...)} *)
X[cs___, 0] := X[cs];
X[] = 1;
X[zeros : (0 ...), c_, cs___] /; c < 0 :=
  X[zeros, -c, Sequence @@ (-{cs})];

(* vectors in Z^infinity *)
V[cs___, 0] := V[cs];
V /: V[cs1___] + V[cs2___] := With[{l1 = {cs1}, l2 = {cs2}},
   With[{l1x = Join[l1, Table[0, Length[l2] - Length[l1]]],
         l2x = Join[l2, Table[0, Length[l1] - Length[l2]]]},
    V @@ (l1x + l2x)]];
V /: n_Integer V[cs___] := V @@ (n {cs});

(* creates a unit vector using the arc id modulo 10 *)
mkV[id_] := With[{label = Mod[id, 10]}, V @@ UnitVector[label, label]];

(* hwhiskers[vec, a, b] is an arc from a to b with whiskers to the left described by vec *)
hwhiskers /: hwhiskers[n_, a_, b_] hwhiskers[m_, b_, c_] := hwhiskers[n + m, a, c];
hwhiskers /: hwhiskers[n_, a_, b_] hwhiskers[m_, c_, b_] := hwhiskers[n - m, a, c];
hwhiskers /: hwhiskers[n_, a_, b_] hwhiskers[m_, a_, c_] := hwhiskers[n - m, c, b];
hwhiskers /: x_hwhiskers^2 := x x;
hwhiskers[n_, a_, a_] := (-A^2 - A^-2) X @@ n;
hwhiskers[n_, a_, b_] /; b < a := hwhiskers[-n, b, a]; (* a normalization *)

hArrowRules = {
  Xp[a_, b_, c_, d_] :>
   A hwhiskers[V[], a, b] hwhiskers[mkV[c] - mkV[d], d, c]
   + A^-1 hwhiskers[mkV[a], d, a] hwhiskers[mkV[b], c, b],
  Xm[a_, b_, c_, d_] :>
   A^-1 hwhiskers[V[], b, c] hwhiskers[mkV[d] - mkV[a], a, d]
   + A hwhiskers[mkV[b], a, b] hwhiskers[mkV[c], d, c]
};

harrow[pd_PD] :=
  (-A^2 - A^-2) (Expand[Times @@ (pd /. hArrowRules)]/(-A^2 - A^-2) //
      FullSimplify // Collect[#, A, Collect[#, _X, Simplify] &] &);
```

Examples:

```
(* Virtual Hopf link *)
In[1]:= harrow[PD[Xm[11, 22, 11, 22]]]
Out[1]= (-(1/A^2) - A^2) (X[1, -1]/A + A X[1, 1])

(* The link in Figure 7 *)
In[2]:= harrow[PD[Xm[82, 31, 72, 21], Xm[72, 41, 62, 31],
                  Xm[21, 52, 11, 82], Xm[11, 62, 41, 52]]]
Out[2]= (-(1/A^2) - A^2) (-A^6 - X[1, -1]^2/A^10 + X[1, -1]^2/A^6 +
```

```
A^2 (1 - X[1, -1]^2) + (-2 + X[1, -1]^2)/A^2)
```

References

[AM] A. A. Akimova and V. O. Manturov, *Labels instead of coefficients: a label bracket which dominates the Jones polynomial, the Kuperberg bracket, and the normalised arrow polynomial*, arXiv:1907.06502v2 [math.GT].

[BK] Hans U. Boden and Homayun Karimi, *The jones-krushkal polynomial and minimal diagrams of surface links*, arXiv:1908.06453v1 [math.GT].

[CKS02] J. Scott Carter, Seiichi Kamada, and Masahico Saito, *Stable equivalence of knots on surfaces and virtual knot cobordisms*, J. Knot Theory Ramifications **11** (2002), no. 3, 311–322, arXiv:math/0008118v1 [math.GT]. MR 1905687

[DJK] Qingying Deng, Xian'an Jin, and Louis H. Kauffman, *On arrow polynomials of checkerboard colorable virtual links*, arXiv:2002.07361v1 [math.GT].

[DK] H. A. Dye and Louis H. Kauffman, *Minimal surface representations of virtual knots and links*, arXiv:math/0401035v5 [math.GT].

[DK09] H. A. Dye and Louis H. Kauffman, *Virtual crossing number and the arrow polynomial*, J. Knot Theory Ramifications **18** (2009), no. 10, 1335–1357, arXiv:http://arxiv.org/abs/0810.3858v3 [math.GT]. MR 2583800

[FK] Lena C. Folwaczny and Louis H. Kauffman, *A linking number definition of the affine index polynomial and applications*, arXiv:1211.1747v1 [math.GT].

[GK] Neslihan Gügümcü and Louis H. Kauffman, *New invariants of knotoids*, arXiv:http://arxiv.org/abs/1602.03579v3 [math.GT].

[Gre04] Jeremy Green, *A table of virtual knots*, 2004, https://www.math.toronto.edu/drorbn/Students/GreenJ/.

[Ima16] Takanori Imabeppu, *On Sawollek polynomials of checkerboard colorable virtual links*, Journal of Knot Theory and Its Ramifications **25** (2016), no. 02, 1650010.

[Kam] Naoko Kamada, *Span of the jones polynomial of an alternating virtual link*, arXiv:math/0412074v1 [math.GT].

[Kam02] Naoko Kamada, *On the Jones polynomials of checkerboard colorable virtual links.*, Osaka J. Math. **39** (2002), no. 2, 325–333 (English).

[Kau99] Louis H. Kauffman, *Virtual knot theory*, European Journal of Combinatorics **20** (1999), no. 7, 663–690. MR 1721925

[Kup03] Greg Kuperberg, *What is a virtual link?*, Algebraic & Geometric Topology **3** (2003), 587–591. MR 1997331

[Mil20] Kyle Miller, *Virtual KnotFolio*, 2020, https://kmill.github.io/knotfolio/.

[Miy06] Yasuyuki Miyazawa, *Magnetic graphs and an invariant for virtual links*, Journal of Knot Theory and Its Ramifications **15** (2006), no. 10, 1319–1334.

[Miy08] Yasuyuki Miyazawa, *A multi-variable polynomial invariant for virtual knots and links*, J. Knot Theory Ramifications **17** (2008), no. 11, 1311–1326. MR 2469206

[Prz] Jozef H. Przytycki, *Fundamentals of Kauffman bracket skein modules*, arXiv:math/9809113v1 [math.GT].

[Tur] Vladimir Turaev, *Knotoids*, arXiv:http://arxiv.org/abs/1002.4133v5 [math.GT].

Department of Mathematics, University of California, Berkeley, California 94720-3840, USA
Email address: kmill@math.berkeley.edu